HAlCl and $AlCl_2$: A Matrix Isolation ESR Study

Ralf Köppe[†] and Paul H. Kasai*

Contribution from the IBM Research Division, Almaden Research Center, 650 Harry Road, San Jose, California 95120-6099

Received August 11, 1995[⊗]

Abstract: Cocondensation of Al atoms and HCl in argon matrices at ∼4 K led to detection by ESR of HAlCl and $AlCl_2$. The ESR spectra observed from the Al/HCl/Argon system are shown; assignments and analyses of the HAlCl and $AlCl_2$ spectra are presented. Both species have a bent form, and the unpaired electron is localized in a nonbonding, sp-hybridized orbital of Al pointing away from the ligand atoms. Ab initio SCF calculations (Gaussian 92) were performed on AlH_2, HAlCl, and $AlCl_2$. The structural features and spin density distributions deduced from the observed hyperfine coupling tensors are in good accord with those given by the SCF calculations. The reaction process between HCl and Al was examined by the MNDO molecular orbital method. The MNDO study indicated that Al and HCl would undergo spontaneously either the insertion reaction, HCl + Al → HAlCl, or the displacement reaction, HCl + Al → H + AlCl, depending on the direction of approach.

Introduction

Spontaneous formation of divalent alumino radicals H−Al−OH upon cocondensation of Al atoms and H_2O in argon matrices was first reported some time ago by Hauge et al.[1] The formation of the insertion product was established by an IR study of the matrices. Knight et al. observed and analyzed later the ESR spectra of H−Al−OH generated in neon and argon matrices.[2] More recently, Howard et al. reported on the formation of the corresponding insertion product H−Al−NH_2 between Al atoms and NH_3 cocondensed in adamantane matrices at 77 K.[3]

For neon matrices in which Al and H_2O were cocondensed, Knight et al. found that subsequent irradiation of matrices with UV (254 nm) resulted in the formation of AlH_2 when H_2O concentration was low (∼0.1%), and generation of $Al(OH)_2$ when the H_2O concentration was high (∼1%). The ESR spectra of AlH_2 and $Al(OH)_2$ thus observed were also analyzed in detail.[4]

We performed an ESR study of reactions between Al atoms and HCl molecules cocondensed in argon matrices. Formation of the expected insertion radical H−Al−Cl was clearly observed for matrices with the HCl concentration of ∼2%. At higher HCl concentration (∼8%), the spectrum was dominated by that of $AlCl_2$. The result is somewhat reminiscent of the photoconversion of H−Al−OH to $Al(OH)_2$ observed in neon matrices with high H_2O content. We also examined matrices in which Al atoms and Cl_2 were cocondensed. The ESR spectrum due to $AlCl_2$ was clearly recognized. The $AlCl_2$ yield here, however, was much poorer than that of the Al/HCl case.

An IR study of Al atoms and Cl_2 molecules cocondensed in argon matrices was reported in an exhaustive study of chemistry of aluminum dichloride by Olah et al.[5] They concluded that, in argon matrices, the initial reaction between Al and Cl_2 is Al + Cl_2 → AlCl + Cl, and higher halides $AlCl_2$ and $AlCl_3$ are formed only from secondary reactions.

We report here (1) the ESR spectra observed from the Al/HCl/Argon system, (2) assignments and analyses of the HAlCl and $AlCl_2$ spectra, (3) results of ab initio SCF calculations performed on AlH_2, HAlCl, and $AlCl_2$, and (4) results of examining the reaction process by the MNDO molecular orbital method. The structural features and spin density distributions deduced from the spin Hamiltonian parameters are in good accord with those predicted by the SCF calculations (Gaussian 92).[6] The MNDO calculations (HyperChem)[7] indicated that the reaction could indeed occur spontaneously and lead to either the insertion reaction, HCl + Al → HAlCl, or the displacement reaction, HCl + Al → H + AlCl, depending on the direction of approach.

Experimental Section

The liquid helium cryostat-ESR spectrometer system that would enable trapping of vaporized metal atoms in an inert gas matrix and examination of the resultant matrix by ESR has been described previously.[8] In the present series of experiments Al atoms were vaporized from a tantalum tube resistively heated to ∼1400 °C, and were condensed in argon matrices mixed with a controlled amount of HCl (1−8%).

The ESR spectrometer used was an IBM Model ER200D system, and a low-frequency (375 Hz) field modulation was used for the signal detection. All the spectra reported here were recorded while the matrix was maintained at ∼4 K, and the spectrometer frequency locked to the sample cavity was 9.428 GHz. Typically 16−64 scans were signal-averaged for an improved signal-to-noise ratio.

Spectra and Assignments

The ground state electronic configuration of Al atoms is $3s^2$-$3p^1$. The ESR signal of Al atoms situated at sites with a cubic

[†] Present address: Universität Karlsruhe, Institut für Anorganische Chemie, Karlsruhe, Germany.

[⊗] Abstract published in *Advance ACS Abstracts,* December 1, 1995.

(1) Hauge, R. H.; Kauffman, J. W.; Margrave, J. L. *J. Am. Chem. Soc.* **1980**, *102*, 6005.

(2) Knight, L. B., Jr.; Gregory, B.; Cleveland, J.; Arrington, C. A. *Chem. Phys. Lett.* **1993**, *204*, 168.

(3) Howard, J. A.; Joly, H. A.; Edwards, P. P.; Singer, R. J.; Logan, D. E. *J. Am. Chem. Soc.* **1992**, *114*, 474.

(4) Knight, L. B., Jr.; Woodward, J. R.; Kirk, T. J.; Arrington, C. A. *J. Phys. Chem.* **1993**, *97*, 1304.

(5) Olah, G. A.; Farooq, O.; Farnia, S. M. F.; Bruce, M. R.; Clouet, F. L.; Morton, P. R.; Prakash, G. K. S.; Stevens, R. C.; Bau, R.; Lammertsma, K.; Suzer, S.; Andrews, L. *J. Am. Chem. Soc.* **1988**, *110*, 3231.

(6) The ab initio calculation was performed using D95** basis sets as implemented in GAUSSIAN 92 (double-ζ quality including one polarization function for each atom). Frisch, K. J.; Trucks, G. W.; Head-Gordon, M.; Gill, P. M. W.; Wong, M. W.; Foresman, J. B.; Johnson, B. G.; Schlegel, H. B.; Robb, M. A.; Replogle, E. S.; Gomperts, R.; Andres, J. L.; Raghavachari, K.; Binkley, J. S.; Gonzalez, C.; Martin, R. L.; Fox, D. J.; Defrees, D. J.; Baker, J.; Stewart, J. J. P.; Pople, J. A. *Gaussian 92*, Revision C; Gaussian, Inc.: Pittsburgh, PA, 1992.

(7) The MNDO program available in HyperChem was used. *HyperChem* (Release 4); Hypercube, Inc.: Waterloo, Ontario, 1994.

(8) Kasai, P. H. *Acc. Chem. Res.* **1971**, *4*, 329.

0002-7863/96/1518-0135$12.00/0

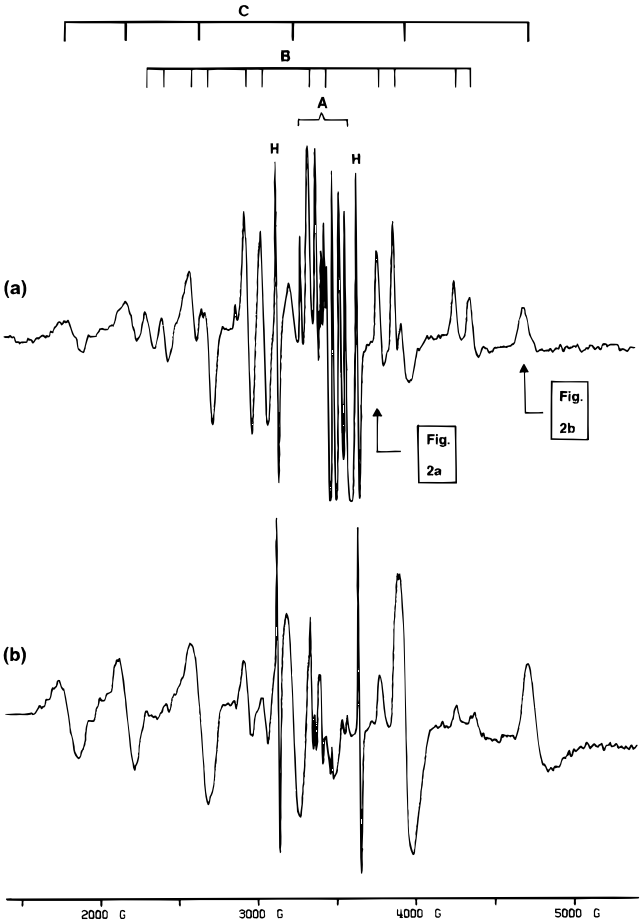

Figure 1. ESR spectra observed from (a) the Al/HCl(2%)/Ar system and (b) the Al/HCl(8%)/Ar system. The doublet indicated by the letter H is due to H atoms. Signals A are due to isolated Al atoms. The sextet-of-doublet B and the sextet C are assigned to HAlCl and $AlCl_2$, respectively.

symmetry would hence be broadened beyond detection owing to the degeneracy of the p orbitals. However, it has been found that rare gas matrices containing a high concentration of Al atoms exhibit strong, well-defined ESR signals. The signals were assigned to Al atoms occupying axially distorted substitutional sites of the host matrix.[9]

Figure 1a shows the ESR spectrum observed from the Al/HCl(2%)/Ar system. The two sharp, isotropic signals indicated by the letter H are the doublet due to hydrogen atoms. Three additional sets of signals, A, B, and C, are recognized as indicated. Signals A are due to Al atoms situated at distorted substitutional sites discussed above. Signals B comprise a sextet of doublets as shown. Signals C are broad and comprise a sextet of larger spacing than that of B. The spectrum similarly observed from the Al/HCl(8%)/Ar system is shown in Figure 1b. It is clearly revealed that an increase in HCl concentration results in diminution of the atomic signals A and the sextet-of-doublets B and dominance of the sextet signals C.

The widely spaced sextet patterns of B and C must surely be attributed to the hfc (hyperfine coupling) interaction with the ^{27}Al nucleus ($I = {}^5/_2$, natural abundance = 100%). The sextet-of-doublet B and the sextet C were thus (tentatively) assigned to the insertion radical, H−Al−Cl, and a secondary radical product, $AlCl_2$, respectively. Closer inspection of individual components revealed partially resolved structures indicative of hf structures due to Cl nuclei, ^{35}Cl ($I = {}^3/_2$, $\mu = 0.82\beta_n$, natural abundance = 75%) and ^{37}Cl ($I = {}^3/_2$, $\mu = 0.68\beta_n$, natural abundance = 25%). The Cl hf structures were best resolved for the second highest field component (of the sextet) of B and the highest field component of C. See Figures 2a and 2b. The resolved structures are consistent with the hfc interactions with one and two chlorine nuclei as indicated, respectively.

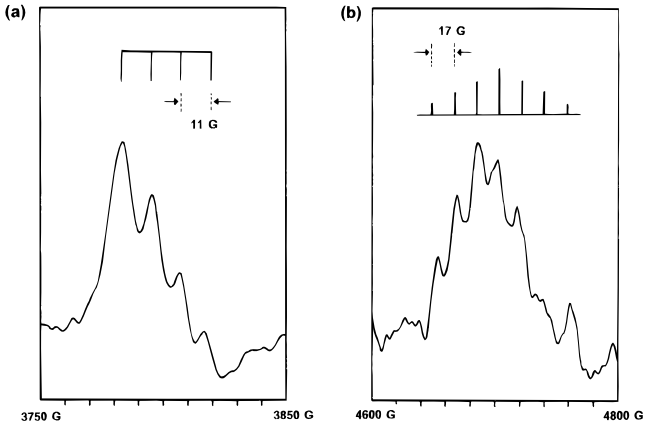

Figure 2. (a) The second highest field component of sextet B and (b) the highest field component of sextet C (of Figure 1a) are shown in an expanded scale. The chlorine hf structures are resolved as indicated.

The sextet splittings due to the Al nucleus observed here are so large that the spectra cannot be analyzed accurately based on the usual second-order solution of the spin Hamiltonian. The **g** tensors and the Al hfc tensors of HAlCl and $AlCl_2$ were hence determined from the resonance positions of the highest and lowest field components and the analytical *continued fraction equations* developed earlier.[10] The proton hfc tensor of HAlCl was assessed directly from the observed doublet splittings.

The assessment of the Cl hfc tensors was not as straightforward. It is expected that HAlCl and $AlCl_2$ both have a bent form, as HAlOH or $Al(OH)_2$, and in each case the unpaired electron is localized in a nonbonding, sp-hybridized Al orbital directed away from the ligand atoms. The Cl hfc interaction of these complexes would then stem from a (small) unpaired electron density in an in-plane Cl 3p orbital(s). The Cl hfc tensors would be approximately axially symmetric, the symmetry axis roughly paralleling the Al−Cl bond. The principal elements of the tensor are then given by $A_{||} = A_{iso} + 2A_{dip}$, and $A_{\perp} = A_{iso} - A_{dip}$.[11] Here A_{dip} represents the anisotropic component related to the spin density in the Cl 3p orbital, and A_{iso} represents the isotropic component related to the spin density in the Cl 3s orbital, or more likely in the present situation, the net manifestation of spin polarization in the doubly occupied valence 3s, and inner 2s and 1s orbitals of the chlorine atom(s). If the polarization process prevails, A_{iso} would be negative. We then note that the only direction along which the principal axes of all the hfc tensors coincide is the direction normal to the molecular plane. The Cl splittings of 11 and 17 G resolved in the spectra of HAlCl and $AlCl_2$ (Figure 2) are hence assigned to the respective perpendicular elements, $A_{\perp}$. A computer program that would simulate the ESR powder pattern of radicals possessing a multiple set of hfc tensors of differing orientations has been described earlier.[12] In order to treat the large, essentially isotropic Al hfc tensor with a better accuracy, the program was modified so that the Al tensor was dealt with by using the Breit−Rabi solution[13] instead of the usual second-

(9) Ammeter, J. H.; Schlosnagle, D. C. *J. Chem. Phys.* **1973**, *59*, 4784.

(10) Kasai, P. H.; McLeod, D., Jr.; Watanabe, T. *J. Am. Chem. Soc.* **1980**, *102*, 179.

(11) Smith, W. V.; Sorokin, P. P.; Gelles, I. L.; Lasher, G. J. *Phys. Rev.* **1959**, *115*, 1546.

(12) Kasai, P. H. *J. Am. Chem. Soc.* **1972**, *94*, 5950.

(13) See, for example, Kopfermann, H. *Nuclear Moments;* Academic Press, New York, 1958, pp 4−41.

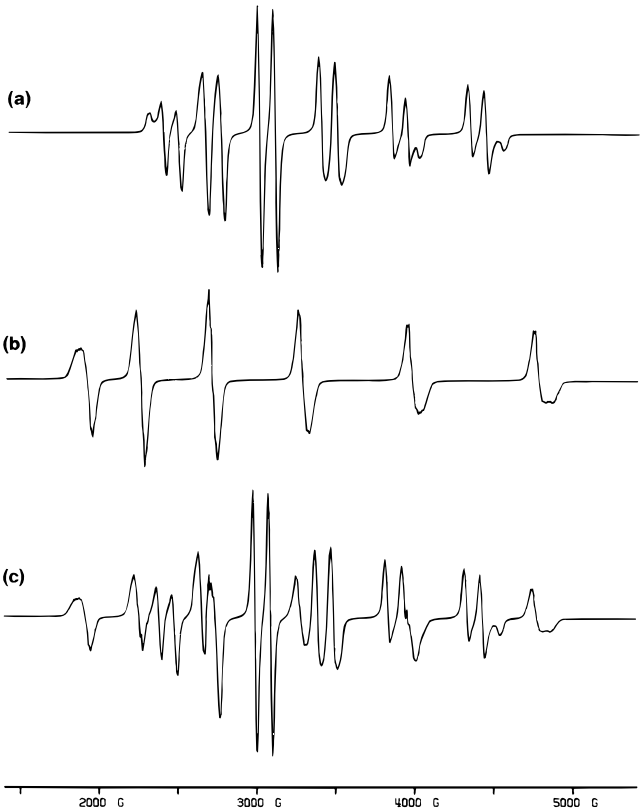

Figure 3. Computer simulated spectra based on the spin Hamiltonian parameters given in Table 1: (a) HAlCl, (b) $AlCl_2$, and (c) a 2/1 mole ratio mixture of HAlCl and $AlCl_2$.

Table 1. The **g** Tensors and the hfc Tensors (given in G) of AlH_2, HAlCl, and $AlCl_2$ Generated in Rare Gas Matrices

molecule	tensor	*z*	*x*	*y*	α[a]
AlH_2/Ne	**g**	2.0026	2.0012	1.9973	
(ref 4)	Al	280	333	281	
	H	44	46	46	
HAlCl/Ar	**g**	1.994(3)	1.991(3)	1.991(3)	
(this work)	Al	385(2)	430(2)	385(2)	
	H	100 (2)	100(2)	100(2)	
	^{35}Cl	−11(1)	0(2)	−11(1)	60°
$AlCl_2$/Ar	**g**	1.992(3)	1.991(3)	1.991(3)	
(this work)	Al	560(2)	600(2)	560(2)	
	^{35}Cl	−17(1)	0(2)	−17(1)	±60°

[a] Molecules lie in the *x*−*y* plane, and for each hfc tensor $A_{||} = A_x$. α denotes the direction of the symmetry axis of the hfc tensor relative to that of the Al hf tensor.

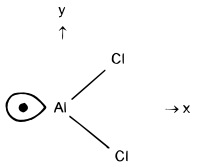

order equation for the resonance field. We then assumed, based on the structures and eigenfunctions given by the ab initio calculations (vide infra), that the symmetry axes of the Cl hfc tensors are oriented ±60° away from the symmetry axis of the Al hfc tensor. Therefrom using the **g** tensor and the Al and proton hfc tensors determined above, the parallel component, $A_{||}$, of the Cl hfc tensors were determined, through an iterative simulation process, as that which would give the best fit with the observed spectrum.

The signs of hfc constants cannot be determined directly from ESR spectra. The large, essentially isotropic Al and H hfc tensors of the HAlCl and $AlCl_2$ radicals indicate substantial unpaired electron densities in the Al and H valence s orbitals. The principal elements of these tensors must hence be positive. The analysis of the Cl hfc tensor delineated above revealed that, for both HAlCl and $AlCl_2$, $|A_\perp| > |A_{||}| \approx 0$. As A_{dip} of the Cl hfc tensor due to an unpaired electron density in a Cl 3p orbital is positive, it must be that the isotropic component, A_{iso}, is negative. The **g** tensors and Al, H, and Cl hfc tensors of HAlCl and $AlCl_2$ thus determined are shown in Table 1. Figures 3a and 3b are the simulated spectra of HAlCl and $AlCl_2$ based on these parameters. Figure 3c shows the result of superposing the HAlCl and $AlCl_2$ spectra with the assumed mole ratio of 2/1. Its agreement with the observed spectrum (Figure 1a) is considered reasonable.

A closer examination of the observed spectra of the Al/HCl/argon system (Figure 1a and 1b) reveals an anomalous change in the relative intensities of individual hf components of the $AlCl_2$ sextet (signals C) with an increase of the HCl concentration (2→8%). It is most clearly noted for the two highest-field components. When molecules are randomly isolated in argon matrices, a certain degree of inhomogeneity of trapping sites is often inevitable. For magnetic molecules with a large, isotropic hfc interaction stemming from an unpaired electron density in an exposed s orbital, such inhomogeneity is manifested as a scatter, Δ*A*, of the hfc constant. The well-known second-order solution for the resonance field of a radical ($S = {}^1/_2$) with one magnetic nucleus is as follows.

$$H(m) = H_0 - mA - \frac{A^2}{2H_0}[I(I+1) - m^2] \qquad (1)$$

where $H_0 = g\beta/(h\nu)$ and $m = m_I$. It follows that an inhomogeneity in *A* given by Δ*A* would produce the inhomogeneity in the resonance field Δ*H*(*m*) as given below.

$$|\Delta H(m)| = \left| m + \frac{A}{H_0}[I(I+1) - m^2] \right| \Delta A \qquad (2)$$

where *A* now represents the most probable isotropic hfc constant.

The effect of trapping site inhomogeneity may thus be incorporated into simulation by adopting the following nuclear level-dependent line width for the ESR signals.

$$W(m) = W_0 + \Delta A \left| m + \frac{A}{H_0}[I(I+1) - m^2] \right| \qquad (3)$$

where W_0 is the intrinsic line width. The spectra shown in Figure 3 were simulated based on the Lorentzian line shape with the intrinsic line width of 10 G and a nil inhomogeneity effect (ΔA = 0 G). Compared in Figure 4 are the ESR spectra of $AlCl_2$ simulated with the m_I-dependent line width of eq 3 with the line width parameters of (a) $W_0 = 10$ G and $\Delta A = 0$ G and (b) $W_0 = 10$ G and $\Delta A = 20$ G.

The latter is in good agreement with the sextet C observed in Figure 1b. It is intriguing that the apparent relative intensities of the hf components may be drastically altered by a small inhomogeneity in *A* of ±2%.

Theoretical Study and Discussions

Structures and SOMO. Included in Table 1 are the **g** tensor and the Al and proton hfc tensors of AlH_2 (in neon matrices) determined earlier by Knight et al.[4] The numbers of valence electrons in AlH_2, HAlCl, and $AlCl_2$ are 5, 11, and 17, respectively. Thus, according to Walsh's rule,[14] they are all

(14) Walsh, A. D. *J. Chem. Soc.* **1953**, 2260−2296.

expected to have a bent structure, and in each case, the semioccupied molecular orbital (SOMO) is given essentially by an sp-hybridized orbital of Al pointing away from the molecule. The Al hfc tensor should hence be axially symmetric with the symmetry axis bisecting the bond angle. The principal elements of the tensor are thus given by $A_{||} = A_{iso} + 2A_{dip}$, and $A_{\perp} = A_{iso} - A_{dip}$, where A_{iso} represents the isotropic component due to the spin density in the Al 3s orbital and A_{dip} represents the anisotropic component due to the spin density in the Al 3p orbital.

Perusing further the bonding scheme of these molecules, one may also predict that the increasing ionicity in the σ bonds in the order of $AlH_2 \rightarrow HAlCl \rightarrow AlCl_2$ should lead to an increase in the p-orbital fraction (hence less electronegativity) of the Al sp-hybridized orbitals involved in the σ bond formation. This then leads to an increase in the s-orbital fraction (and the associated decrease in the p-orbital fraction) in SOMO, the nonbonding Al sp-hybridized orbital. A_{iso}(Al) indeed increases conspicuously from 300 G for AlH_2 to 600 G for $AlCl_2$, while the anisotropy, $A_{||}$(Al) − $A_{\perp}$(Al), decreases from 53 to 40 G. These values may be compared with the isotropic hfc constant, $A°_{iso}$(Al) = 1400 G, computed for a unit spin density in the Al 3s orbital, and the anisotropy of the hfc tensor, $A°_{||}$(Al) − $A°_{\perp}$(Al) = $3A°_{dip}$(Al) = 90 G, computed for a unit spin density in the Al 3p orbital.[15] As for the proton hfc constant, it may be compared with the hfc constant, $A°_{iso}$(H) = 505 G, of hydrogen atoms isolated in argon matrices.[16] The anisotropy of the hfc tensor computed for a unit spin density in the Cl 3p orbital, $A°_{||}$(Cl) − $A°_{\perp}$(Cl) = $3A°_{dip}$(Cl), is 189 G.[15] Based on these "atomic values" the unpaired electron densities in the relevant valence orbitals in SOMO's of AlH_2, HAlCl, and $AlCl_2$ were deduced as follows. The sum of densities thus determined is

molecules	Al(3s)	Al(3p)	H(1s)	Cl(3p)	Σ(density)
AlH_2	0.21	0.59	0.09		0.98
HAlCl	0.28	0.50	0.20	0.06	1.04
$AlCl_2$	0.41	0.44		0.09	1.03

reasonably close to a unit in each case. The bond angles X−Al−X of these triatomic molecules may be deduced from the remaining in-plane Al p orbitals. The angles thus deduced are 115°, 109°, and 106° for AlH_2, HAlCl, and $AlCl_2$, respectively.

In order to gain further elucidation on the structural and molecular orbital aspects of these molecules, we performed ab initio SCF calculations.[6] $AlCl_3$ and AlCl species were also examined. The structural results and the Al−Cl stretching frequencies (for $AlCl_{n=1,2,3}$) thus obtained are shown in Table 2. In the series HAlCl/AlCl → $AlCl_2$ → $AlCl_3$ the ionic contribution to bonding increases with increasing number of electronegative Cl ligands. The effect is manifested in shortening of the Al−Cl bond, and associated increase of the Al−Cl stretching frequency. The calculated bond angle decreases (slightly) from AlH_2 to HAlCl, but then increases for $AlCl_2$. The trend is at discord with the bond angle changes deduced from the sp-hybridization of the central Al atom. The discrepancy may be attributed to the repulsive interaction between the negatively charged Cl atoms.

The isotropic component of a hfc tensor is related to the Fermi contact term as follows:[11] $A_{iso} = (8\pi/3)g_e\beta_e g_n\beta_n|\Phi(0)|^2$. The Fermi contact terms $|\Phi(0)|^2$ determined from the observed hfc tensors and those given by the ab initio calculations are compared in Table 3. In spite of the relatively low level of

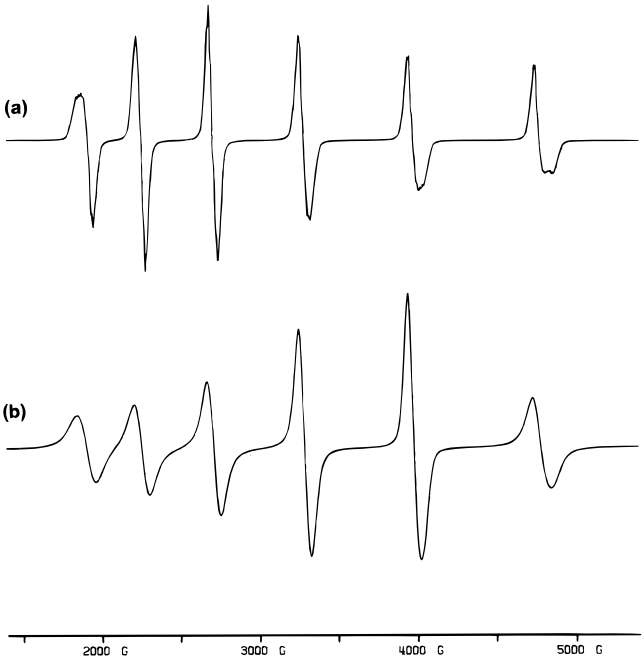

Figure 4. ESR spectra of $AlCl_2$ simulated with the nuclear level dependent line width of eq 3: (a) W_0 = 10 G and ΔA = 0 G, and (b) W_0 = 10 G and ΔA = 20 G. See text for details.

Table 2. Theoretical Results Obtained from ab Initio SCF Calculations (GAUSSIAN 92, Basis Set D95**, UHF If Open Shell, Otherwise RHF; *r* in Å, and Bond Angles in deg)

parameters	AlH_2	HAlCl	$AlCl_2$	$AlCl_3$	AlCl
symmetry	C_{2V}	C_s	C_{2V}	D_{3h}	
r (Al−H)	1.591	1.587			
r (Al−Cl)		2.131	2.116	2.082	2.165
bond angle	118.2	116.0	117.9	120.0	
ν (Al−Cl) (IR) (obsd)[a]			587.1 (563.6)	642.1 (619.2)	478.8 (455.2)

[a] In cm^{-1}. Observed data are from ref 5.

Table 3. The Fermi-Contact, $|\Phi(0)|^2$: Theoretical and Experimental (Determined from the Observed A_{iso}'s) Values (in au)

			$\|\Phi(0)\|^2$	
molecule	nucleus	obsd	all s's	valence s
AlH_2/Ne	Al	0.717	0.675	0.909
(ref 4)	H	0.029	0.028	0.026
HAlCl/Ar	Al	0.962	0.892	1.172
(this work)	H	0.063	0.056	0.053
	^{35}Cl	0.047	0.066	0.007
$AlCl_2$/Ar	Al	1.379	1.306	1.749
(this work)	^{35}Cl	0.072	0.094	0.009

calculations for the open-shell systems (no electron correlation) a good overall agreement is seen between the experimental and theoretical values. The table also shows $|\Phi(0)|^2$, given by the ab initio calculations, due to the unpaired electron densities in the respective valence s orbitals. It is revealed that for the Al nucleus the Fermi contact term from the valence s orbital is ∼30% larger than the total $|\Phi(0)|^2$. Analysis of the gross orbital population showed that the difference is due to negative spin densities in the inner 1s and 2s orbitals. For the Cl hfc tensors, however, the total contact term is ∼10 times larger than the value due to the valence s orbital. Gross orbital population analyses of HAlCl and $AlCl_2$ showed the presence of a net negative spin density in each of the doubly occupied valence and inner s orbitals of the Cl atom(s). The calculations thus

(15) Morton, J. R.; Preston, K. F. *J. Magn. Reson.* **1978**, *30*, 577.
(16) Foner, S. N.; Cochran, E. L.; Bowers, V. A.; Jen, C. K. *J. Chem. Phys.* **1960**, *32*, 963.

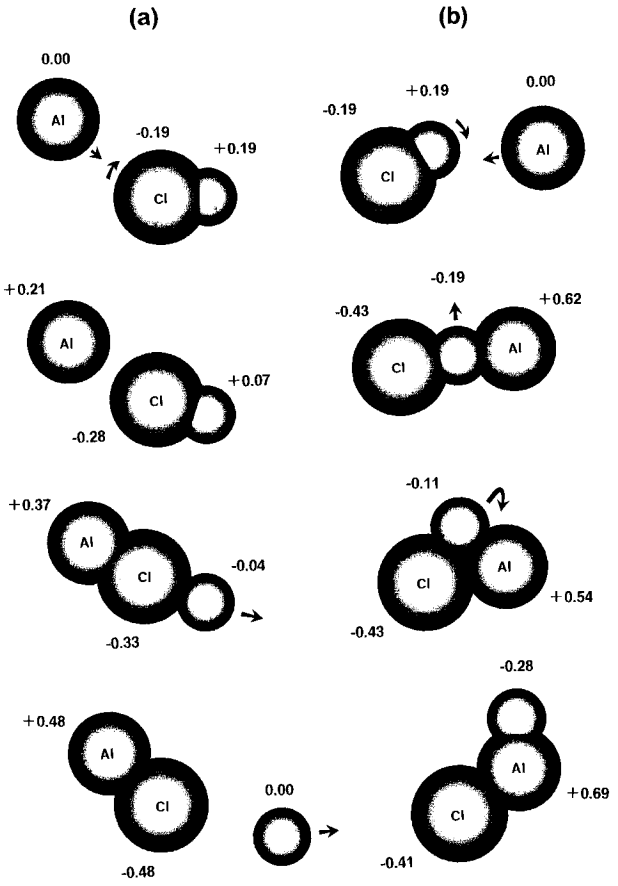

Figure 5. Several sequential stages predicted by MNDO for the triatomic system HCl/Al undergoing: (a) the displacement reaction HCl + Al → H + AlCl and (b) the insertion reaction HCl + Al → HAlCl. The atomic charges at each state are also shown.

revealed that the Cl A_{iso}'s of HAlCl and $AlCl_2$ are indeed negative, and are due mostly to polarization in the inner s orbitals.

Reaction Process. Al atoms thus appear to have a unique propensity to undergo an insertion reaction. In addition to the Al/H_2O and Al/NH_3 cases discussed earlier,[1−3] the insertion reaction has also been observed for Al atoms and alkyl ethers cocondensed in hydrocarbon matrices at 77 K.[17] In every case it has been concluded that ground state Al atoms react spontaneously to produce the insertion product(s). In all of these experiments Al atoms were generated either from a Knudsen cell heated to ∼1400 °C or by laser sputtering. In the experiment by Knight et al., for the formation of HAlOH by the laser method, H_2O vapor was introduced directly above the Al target.[2] We decided to examine, at the level of the MNDO MO theory, whether the reaction between HCl and Al would

(17) Chenier, J. H. B.; Howard, J. A.; Joly, H. A.; LeDuc, M.; Mile, B. *J. Chem. Soc., Faraday Trans.* **1990**, *86*, 3321.

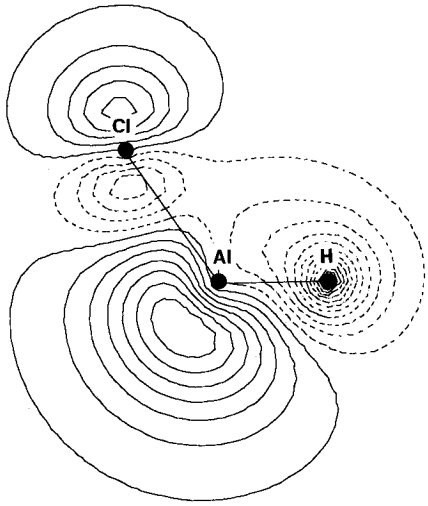

Figure 6. The contour plot (in the molecular plane) of SOMO of HAlCl given by MNDO.

proceed spontaneously. The MNDO method available in HyperChem was used.[7] The HCl diatomic system was first geometry optimized. Then an Al atom was placed ∼5 Å away from the HCl system and the geometry optimization was performed on the triatomic system. The method of steepest decent was used to follow the energy surface trough. With a relatively fast PC (a Pentium 90 MHz model) the entire reaction sequence was completed (with simultaneous molecular model monitoring) within several minutes.

The MNDO examination thus performed predicted that HCl and Al indeed react spontaneously at their ground states, and most interestingly that the insertion reaction, HCl + Al → HAlCl, occurs when the Al atom is placed on the hydrogen side of HCl, while the displacement reaction, HCl + Al → H + AlCl, occurs when Al is placed on the chlorine side. The insertion reaction is the dominating process. The displacement reaction occurred only when the Al atom was placed within the ±∼50° conical space centered about the H−Cl bond. Several exemplary stages of reaction predicted for the respective sequences are shown in Figure 5. The atomic charges at each state are also shown. It is seen that the interaction responsible for either reaction sequence is that of charge transfer. The Al → H charge transfer interaction is clearly the initial driving force for the insertion sequence. The contour plot of SOMO of HAlCl (of the final geometry) given by MNDO is shown in Figure 6. The valence orbitals involved and the extent of Al → H charge transfer within SOMO are clearly revealed.

Acknowledgment. Ralf Köppe is grateful for the financial support of Deutsch Forschungsgemeinschaft for his stay at IBM Almaden Reset Center.

JA952736F